General Disclaimer

One or more of the Following Statements may affect this Document

- This document has been reproduced from the best copy furnished by the organizational source. It is being released in the interest of making available as much information as possible.

- This document may contain data, which exceeds the sheet parameters. It was furnished in this condition by the organizational source and is the best copy available.

- This document may contain tone-on-tone or color graphs, charts and/or pictures, which have been reproduced in black and white.

- This document is paginated as submitted by the original source.

- Portions of this document are not fully legible due to the historical nature of some of the material. However, it is the best reproduction available from the original submission.

(2)

THE ELECTROMAGNETIC FORCE FIELD, FLUID FLOW FIELD AND TEMPERATURE PROFILES IN LEVITATED METAL DROPLETS

by

N. El-Kaddah and J. Szekely

NSG- [illegible]

(NASA-CR-169071) THE ELECTROMAGNETIC FORCE FIELD, FLUID FLOW FIELD AND TEMPERATURE PROFILES IN LEVITATED METAL DROPLETS (Massachusetts Inst. of Tech.) 39 p HC A03/MF A01 CSCL 11F G3/26

N82-26437

Unclas 24018

Department of Materials Science and Engineering
Massachusetts Institute of Technology
Cambridge, Massachusetts 02139

ABSTRACT

A mathematical representation has been developed for the electromagnetic force field, the fluid flow field, the temperature field (and for transport controlled kinetics), in a levitation melted metal droplet. The technique of mutual inductances was employed for the calculation of the electromagnetic force field, while the turbulent Navier - Stokes equations and the turbulent convective transport equations were used to represent the fluid flow field, the temperature field and the concentration field. The governing differential equations, written in spherical coordinates, were solved numerically.

The computed results were found to be in good agreement with measurements reported in the literature, regarding the lifting force, and the average temperature of the specimen and carburization rates, which were transport controlled.

1. INTRODUCTION

The levitation melting technique, that is the positioning of metal droplets by an electromagnetic force field, generated by induction coils of suitable geometry has gained a great deal of popularity during the 1950's and 1960's. The principal attraction of this technique was that small metallic samples (say ranging in weight from .5 to 5 g.) could be melted and reacted in the absence of a solid container. It was generally held that the eddy currents induced in the metallic sample produced a spatially uniform temperature field thus the technique was found to be particularly useful for studying gas - melt interactions.

More recently levitation melting is gaining rather greater prominence, because electromagnetic force fields are being used for the positioning of samples in space processing experiments. One of the important features of these systems is that the absence of gravity will necessarily eliminate thermal buoyancy driven natural convection, a factor, of particular importance in certain solidification studies. However, since the samples are positioned by an electromagnetic force field, the question will naturally arise whether this force field in itself may give rise to convection currents, furthermore whether any temperature gradients that may exist on the free surface of these samples may give rise surface tension driven flows.

Clearly, a quantitative understanding of these phenomena would be highly desirable, for both the planning and the interpretation of in-flight experiments. Furthermore, the quantitative description of the temperature and velocity fields in levitated droplets under conventional ground based experimental conditions would also be of considerable interest, since this knowledge would be very helpful in the interpretation of any kinetic measurements.

Previous work in the area of levitation melting may be divided into two categories, namely experimental studies concerned with physico-chemical measurements at high temperatures, which did not consider transport phenomena in the melt on the one hand, [1] and purely electrodynamic work, concerned with the calculation of the lifting force on the other. [2]

The principal purpose of the present paper is to develop the theoretical framework for combining the electrodynamic and the transport aspects of this problem.

2. FORMULATION

Fig. 1 shows a sketch of the conventionally used coil arrangements for the levitation melting of metal droplets. It is seen that an AC current is being passed through two (or more) opposing coils and as a result an electromagnetic force field is being generated.

This force field will have two effects on a metallic specimen located between the coils:

(i) A net force (lifting force) will be exerted on the specimen, which, when large enough compared to the weight of the sample, will be able to balance the gravitational force and thus "levitate the specimen".

(ii) The induced eddy currents dissipated in the sample will cause "Joule Heating" and will also generate a stirring force.

In developing a quantitative representation of such a system, one has to

(a) Calculate the electromagnetic force field acting on the specimen, hence the lifting force, i.e. the conditions for levitation for a given applied magnetic field, such as the coil current and the coil configuration.

(b) Calculate the fluid flow field, as generated by the electromagnetic (Lorentz) forces.

(c) Calculate the temperature field that results from the balance between heat generation and heat dissipation due to convection and radiation.

Here one should remark that the governing equations are necessarily coupled, because the fluid flow within the sphere is driven by the combined effects of thermal natural convection and electromagnetic forces. Furthermore, the spatially variable heat generation in the system is caused by the current distribution. While a number of electromagnetically driven flow problems have been successfully modelled in the past,[3-7] the present system poses the additions complication of spherical symmetry.

2.1 Calculation of the Electromagnetic Force Field and of the Lifting Force

Let us consider a molten sphere having spatially uniform physical properties sketched in Fig. 2. Let us consider furthermore, that the applied electromagnetic force field also shown in the figure will be axially symmetrical. For spherical geometry the induced current will be flowing in the ϕ direction.

The induced current will generate a magnetic field and the interaction of this magnetic field with the current will give rise to an electromagnetic force field.

These electric phenomena will have three manifestations:

(a) A lifting force will be generated

(b) Thermal energy will be dissipated in the metallic speciman

(c) A stirring force will be exerted on the specimen.

F_ℓ, the total levitation force is given by

$$\underset{\sim}{F}_\ell = \int_V (1/2)\,\mathrm{Re}\,(\underset{\sim}{J}\times\underset{\sim}{B}_a^*)\,dv \qquad (1)^{**}$$

furthermore the power adsorbed by the melt (i.e. the total Joule Heat generated) is:

$$P = \int_V (1/2)\mathrm{Re}(\underset{\sim}{J}\cdot\underset{\sim}{J}^*)/\sigma\,dv \qquad (2)$$

finally the spatial distribution of the time-averaged stirring force in the melt per unit volume is:

$$\underset{\sim}{F}_s = 1/2)\,\mathrm{Re}\,(\underset{\sim}{J}\times\underset{\sim}{B}^*) \qquad (3)$$

**The list of symbols is given at the end of the paper.

What needs to be done here is to evaluate the induced current density $\underset{\sim}{J}$ and the magnetic flux intensity $\underset{\sim}{B}$, for a given coil geometry and coil current.

In essence there are two ways in which this may be accomplished. One of these would involve starting with the differential Maxwell's equations, solving for the magnetic field and then computing the induced current. (6)

The alternative technique, which will be used here, involves the concept of mutual inductances. In this integral formulation the specimen (i.e. the levitated droplet) is considered to consist of a set of electrical circuits and one solves for the current generated in each of these. Once the current distribution is known, the magnetic flux density is readily calculated and hence the terms appearing in Eqs. (1)-(3) may be evaluated.

The magnetic flux density $\underset{\sim}{B}$ for a given current distribution is given by Ampere's law:

$$\underset{\sim}{B} = \frac{\mu_o}{4\pi} \int_{vol} \frac{\underset{\sim}{J} \times \hat{a}_r}{r'^2} \, dv \qquad (4)$$

where $\underset{\sim}{J}$ is the current density in a volume element dv at a distance r' from the point at which the flux density $\underset{\sim}{B}$ is being evaluated and $\hat{a}_r$ is the unit vector in the r direction. The quantity $\underset{\sim}{J}$ must include the induced current within the levitated sphere as well as the current within the coil.

Let us define the vector potential $\underset{\sim}{A}$, as:

$$\underset{\sim}{B} = \underset{\sim}{\nabla} \times \underset{\sim}{A} \qquad (5)$$

Then Eq. (4) becomes

$$\underset{\sim}{A} = \frac{\mu_o}{4\pi} \int_{vol} \frac{\underset{\sim}{J}}{r'} \, dv \qquad (6)$$

On noting the axial symmetry of the field, the levitated

sphere is divided into elementary circuits as shown in Fig. (3). Each segment of the spherical shell is considered as a region of constant current density. For such a system Eq. (6) may be written as:

$$A_\phi = \frac{\mu_o}{4\pi} \left\{ \sum_{c=1}^{\text{sphere}} (J.S)_c \oint \frac{d\ell_s}{r'} + \sum_{k=1}^{\text{coils}} I(k) \oint \frac{d\ell_k}{r'} \right\} \qquad (7)$$

where $d\ell$ is the line element of circuit of constant current density, and S is the cross sectional area of the circuit, and I(k) is the coil current

It should be noted that first term on the rhs of Eq. (7) describes the induced potential while the second term describes the applied potential.

From Faraday's law of induction, the induced current in anv circuit, i in a levitated sphere is given explicitly by:

$$\oint E_i . d\ell_i = - \frac{d}{dt} \int_s B . ds \qquad (8)$$

where the surface of integration is bounded by the periphery of the circuit.

For a time harmonic field we have

$$J = \text{Re} \{ J \; e^{j\omega t} \} \qquad (9)$$

$$B = \text{Re} \{ B \; e^{j\omega t} \} \qquad (10)$$

Using Eq. (9) - (10), Eq. (8) can be written as:

$$\oint J_i . d\ell_i = -j\omega\sigma \left\{ \sum_{c=1}^{\text{sphere}} M_{i,c} (J.S)_c + \sum_{k=1}^{n} M_{i,k} I(k) \right\} \qquad (11)$$

where

$$M_{i,c} = \frac{\mu_o}{4\pi} \oint \oint \frac{d\ell_i d\ell_c}{r'} \qquad (12)$$

is the mutual inductance, (on self inductance, when i=C) which may be calculated using the ring-ring formulas (8).

Finally in order to avoid dealing with complex numbers, equation (12) is separated into real and imaginary parts, as follows:

The levitated sphere depicted in Fig. (8) is divided into N x L circuits. The eddy current distribution can be obtained by solving 2 x N x L real, simultaneous algebraic equations.

$$\sigma\omega \sum_{\mu=1}^{N} \sum_{\nu=1}^{L} M_{(i,\ell),(\mu,\nu)} \, \mathrm{Re}\,(J.S)_{(\mu,\nu)} + \mathrm{Im}\,(J_{(i,\ell)} 2\pi r \sin\theta \qquad (13)$$

$$= -\sigma\omega \sum_{k=1}^{\text{coils}} M_{(i,\ell)\,k} \, \mathrm{Re}(I_k)$$

$$\sigma\omega \sum_{\mu=1}^{N} \sum_{\nu=1}^{L} M_{(i,\ell),(\mu,\nu)} \, \mathrm{Im}(J.S)_{\mu,\nu} - \mathrm{Re}\; J_{i,\ell}\, 2\pi r \sin\theta$$

$$= \omega\sigma \sum_{k=1} M_{(i,\ell),k} \, \mathrm{Im}\,(I_k) \qquad (14)$$

In the present case, the vector potential has only one component, in the ϕ direction; since the vector potential has the same direction as the current, B_r, and B_θ are related to $\underset{\sim}{A}$ as follows:

$$B_r = \frac{1}{r \sin\theta} \frac{\partial}{\partial\theta} (A_\phi \sin\theta) \qquad (15)$$

$$B_\theta = \frac{1}{r} \frac{\partial}{\partial r} (r A_\phi) \qquad (16)$$

Thus finally the knowledge of B_r, B_θ and J_ϕ enables one to evaluate the quantities F_ℓ, P and F_s which were defined in Eqs. (1-3).

2.2 Calculation of the Fluid Flow Field

In general the fluid flow field in levitated metal droplets will be driven by two forces, that is the electromagnetic force field (which we have just calculated) and the buoyancy force field, which is due to temperature differences within the specimen. It may be expected that the velocity field will be turbulent, so that appropriate techniques have to be invoked for evaluating the turbulent shear stresses (i.e. the Reynolds stresses).

The following principal assumptions are made in the development of the governing equations.

(1) The flow field will be considered to be two dimensional, that is only the r and the θ components of the velocity will appear.

(2) The k-ε model[9,10] may be used to represent the turbulent viscosity

(3) Any possible damping of the turbulence by the magnetic field is neglected

(4) No allowance is made either for the anisotropy of turbulence near the free surface, or for the possible damping effect due to surface tension forces near the free surface.

On commenting on the appropriateness of these assumptions it is noted that because of the axial symmetry (symmetrical location of the specimen regarding the coils) the assumption concerning the two dimensional nature of the velocity field was thought to be reasonable.

The k-ε model has been selected because this has been a quite widely used approach for modelling turbulent electromagnetically driven flows[11,12], with considerable success and at present there appears to be no obvious, more satisfactory alternative.

The last two assumptions represent an oversimplification, which ought to be refined, once experimental data become available in order to permit this. The implications of these assumptions, in the light of some experimental measurements, will be discussed subsequently.

For steady two dimensional flow in spherical coordinates, the governing equations take the following form:

The equation of continuity:

$$\frac{1}{r^2}\frac{\partial}{\partial r}(\rho r^2 U_r) + \frac{1}{r \sin\theta}\frac{\partial}{\partial \theta}(\rho U_\theta \sin\theta) = 0 \qquad (17)$$

The equation of motion:

r direction

$$\frac{1}{r^2}\frac{\partial}{\partial r}(\rho U_r^2 r^2 - \mu_{eff} r^2 S_{rr}) + \frac{1}{r \sin\theta}\frac{\partial}{\partial \theta}(\rho U_r U_\theta \sin\theta - \mu_{eff} \sin\theta\, S_{r\theta}) = SU_r \qquad (18)$$

θ direction

$$\frac{1}{r^2}\frac{\partial}{\partial r}(\rho U_r U_\theta r^2 - r^2 \mu_{eff} S_{r\theta}) + \frac{1}{r \sin\theta}\frac{\partial}{\partial \theta}(\rho U_\theta \sin\theta - \mu_{eff} \sin\theta\, S_{\theta\theta}) = SU_\theta \qquad (19)$$

where S_{ij} is the symmetric part of the strain rate tensor

$$SU_r = \frac{U_\theta^2}{r} - \frac{\partial \bar{p}}{\partial r} - \mu_{eff}\left(\frac{S_{\theta\theta}+S_{\phi\phi}}{r}\right) - (\rho-\rho_0) g \sin\theta + \frac{1}{2}\rho Re\,(J_\phi B_\theta^*) \qquad (20)$$

$$SU_\theta = -\frac{U_r U_\theta}{r} - \frac{1}{\rho}\frac{\partial \bar{p}}{\partial \theta} + \mu_{eff}\frac{S_{r\theta}}{r} - \frac{\cot\theta}{r}\mu_{eff}S_{\phi\phi}$$

$$+ (\rho-\rho_0)\, g\cos\theta + \frac{1}{2}\rho R_e (J_\phi B_r^*) \qquad (21)$$

where

$$\bar{p} = p - \rho_0 gr\cos\theta \qquad (22)$$

$$\rho = \rho_0(1 - \alpha\nabla T) \qquad (23)$$

$$S_{rr} = \frac{\partial U_r}{\partial r} \qquad (24)$$

$$S_{\theta\theta} = \frac{1}{r}\frac{\partial U_\theta}{\partial \theta} + \frac{U_r}{r} \qquad (25)$$

$$S_{\phi\phi} = \frac{U_r}{r} + \frac{U_\theta \cot\theta}{r} \qquad (26)$$

$$S_{r\theta} = \frac{1}{2}\left\{r\frac{\partial}{\partial r}\left(\frac{U_r}{r}\right) + \frac{1}{r}\frac{\partial U_r}{\partial \theta}\right\} \qquad (27)$$

The turbulent or eddy viscosity may be calculated by using the k-ε model:

$$\mu_t = C_\mu \rho k^2/\varepsilon \qquad (28)$$

Separate transport equations will have to be written for k, the turbulent kinetic energy and ε the turbulent kinetic energy dissipation; these take the following form:

The turbulent kinetic energy:

$$\frac{1}{r^2}\frac{\partial}{\partial r}\left(\rho U_r r^2 k - r^2\left(\mu + \frac{\mu_t}{\sigma_k}\right)\frac{\partial k}{\partial r}\right) - \frac{1}{r\sin\theta}\frac{\partial}{\partial \theta} \qquad (29)$$

$$\left(\rho U_\theta \sin\theta\, k - \left(\mu + \frac{\mu_t}{\partial k}\right)\frac{\sin\theta}{r}\frac{\partial k}{\partial \theta}\right) = SU_k$$

where

$$SU_k = 2\mu_t (S_{rr}^2 + S_{00}^2 + S_{\phi\phi}^2 + S_{r0}^2) - \rho\varepsilon \tag{30}$$

The turbulent energy dissipation:

$$\frac{1}{r^2} \frac{\partial}{\partial r} (\rho U_r r^2 \varepsilon - r^2 (\mu + \frac{\mu_t}{\sigma\varepsilon}) \frac{\partial \varepsilon}{\partial r}) - \frac{1}{r \sin\theta}$$

$$\frac{\partial}{\partial \theta} (\rho U_\theta \sin\theta \, \varepsilon - (\mu + \frac{\mu_t}{\sigma\varepsilon}) \frac{\sin\theta}{r} \frac{\partial \varepsilon}{\partial \theta} = SU_\varepsilon \tag{31}$$

where

$$SU_\varepsilon = 2C_1 \frac{\varepsilon}{k} \mu_t (S_{rr}^2 + S_{00}^2 + 2S_{\phi\phi}^2 + S_{r\theta}^2)$$

$$- C_2 \rho \frac{\varepsilon^2}{k} \tag{32}$$

and σ_k, σ_ε, C_μ, C_1 and C_2 are constants. At high values of the Reynolds number all these quantities are generally assumed to be constant. At low Reynolds numbers C_μ and C_2 will become dependent on $Re_T = k^2/\nu\varepsilon$). The values of these constants and of the function are given elsewhere.[9,10]

2.3 Temperature field

The temperature field in a levitated metal droplet is governed by the rate of heat generation, due to Joule Heating, the rate of convective and radiative loss from the free surface and by the rate at which thermal energy is being transported inside the specimen, by conduction and by convection.

Written in spherical coordinates the convective energy balance equation takes the following form:

$$\frac{1}{r^2}\frac{\partial}{\partial r}\left(\rho\ r^2 T - U_r^2\left(\frac{\mu}{p_{r\ell}} + \frac{\mu_t}{p_{rt}}\right)\frac{\partial T}{\partial r}\right) - \frac{1}{r\sin\theta}$$

$$\frac{\partial}{\partial\theta}\left(\rho U_0 \sin\theta T - \frac{\sin\theta}{r}\left(\frac{\mu}{pr_\ell} + \frac{\mu_t}{pr_t}\right)\frac{\partial T}{\partial\theta}\right) = \frac{Re\ (J, J^*)}{2\sigma C_p} \tag{33}$$

The boundary conditions necessary to complete the statement of the problem are given as follows:

At the axis of symmetry $\theta = 0$ and $\theta = \pi$

$$\left.\begin{aligned} U_0 &= 0 \\ \partial U_r/\partial\theta &= 0 \\ \partial k/\partial\theta &= 0 \\ \partial\varepsilon/\partial\theta &= 0 \\ \partial T/\partial\theta &= 0 \end{aligned}\right\} \quad \text{Statement of symmetry.} \tag{34}$$

At the surface of sphere $r = R$

$$\left.\begin{aligned} \partial U_0/\partial r &= 0 \\ U_r &= 0 \\ \partial k/\partial r &= 0 \\ \partial\varepsilon/\partial r &= 0 \\ -k\frac{\partial T}{\partial r} &= h\ (T - T_b) + \sigma\varepsilon(T^4 - T_b^4) \end{aligned}\right. \tag{35}$$

These surface boundary conditions express the physical constraints that momentum, turbulent kinetic energy and the rate of turbulent energy dissipation are not transported across the phase boundary, and that the velocity normal to the phase boundary is zero.

The last equation expresses the continuity of the heat flux.

h, the convective heat transfer coefficient between the levitated drop and the surrounding gas stream was correlated for forced convection and natural convection as [13].

$$Nu = 0.8 Re^{1/2} Pr^{1/3} \qquad 150 < Re < 500 \qquad (36)$$

$$Nu = 0.78 (Gr\ Pr)^{1/4} \qquad 10^5 < Gr < 10^8 \qquad (37)$$

3. COMPUTATIONAL TECHNIQUE

In generating a solution of the governing equations the magnetic field equations were solved first. This involved dividing the sphere into 8x15 circuit elements and solving the resultant set of linear equations. Once the current distribution was known, the magnetic flux density was readily calculated, together with the electromagnetic force field vector, the pattern of Joule Heat generation and the lifting force.

In the subsequent phase of the computation the fluid flow equations, the convective heat flow equation and the conservation equations for k and ε were solved together, using a finite difference technique described by Spalding. [14]

A 10x17 grid structure was used and the computation required about 100 seconds on MIT's IBM 370 digital computer.

4. COMPUTED RESULTS

In the following we shall present a selection of the computed results, pertaining to the lift force exerted on levitated droplets, on the fluid flow and heat flow phenomena and finally this information will be used for the interpretation of some measurements, obtained by one of the authors on the carburization of molten iron droplets. [13,15]

The actual calculations were carried out for input parameters which correspond to the experimental conditions used for these carburization measurements. One gram of iron was levitated in a CO_2+CO gas mixture, at 40 atmospheres, with a gas flow rate of 5 l/m (STP). The tube containing the droplet and the gas stream was 13 mm in diameter. Under steady state conditions the temperature of the molten drop was 1650°C.

The actual coil configuration used is given in Fig. 1; the coils were made of silver tubing, 3.1 mm in diameter. Two co-planar turns, 17.2 mm inner diameter were employed, both above and below the levitated sphere. The distance between the upper and the lower turns was 10 mm.

The power supply was a 10kW, 450 kHz high frequency generator. The actual coil current was not measured, but its value will be deduced from subsequent heat flow calculations.

4.1 Lift Force Calculations

In order to find the position of the levitated sphere, for an estimated coil current, the lifting force and power absorbed is calculated along the axis of the coil. Figs. (4) to (6) show the results for coil currents of 200, 250, 300 Amp respectively. The symmetry of the force field and power absorption around the center of the coil is a result of the symmetry of coil. At a 200 Amp coil current, Fig. (4), the maximum lifting force is 7×10^{-3} N which is less than weight of the drop (9.81×10^{-3}N). Under these conditions it is not possible to levitate the 1 gram iron drops. At higher coil currents Figs. (5) and (6) levitation is possible as indicated by the intersection of the curves representing the lift force (F_ℓ) and the weight of the particle (mg). There are two positions where the electromagnetic force balances the

weight of the drop, as clearly shown in Fig. (5), but only the larger of these two values does correspond to a stable equilibrium, since any upward or downward deviation from it produces a restoring lifting force decrement or increment respectively. It is interesting to note that at zero gravity, the stable position corresponds to the center of the coil. The power absorbed at 250 was 70 W while for 300 this figure was 51W. The decrease of the power absorption by increasing coil current is the basic feature of electromagnetic levitation.

The coil current may now be estimated with reasonable accuracy, because a value of about 250A will give the proper lifting force. Furthermore, as will be shown subsequently, the corresponding power input will give the correct droplet temperature, using an overall energy balance.

4.2 Electromagnetic forces and heat generation in levitated sphere.

Fig. (7) shows the computed force field and the heat generation pattern in the drop. It is seen that the electromagnetic field is markedly attenuated beyond the skin depth which is 0.9 mm for molten iron at 450 KHz. As a result of positioning the levitated sphere close to to the bottom coils the force field and heat generation are moved toward the lower half of the sphere.

Since the current only penetrates a very small region in the drop, the magnetic flux density increases rapidly with r as it approaches to the surface, therefore the electromagnetic forces are almost normal to the r direction.

4.3 Flow Fields

The computed velocity field and temperature field are given in Fig. (8) . The computed velocity field shows a double loop circulation pattern, which is consistent with the force field shown in the previous figure and is to be expected for a stationary electromagnetic field. The maximum velocity at the free surface was found to be about 0.28 m/s, which is in reasonable qualitative agreement with measurements reported in the literature. More specifically Robertson estimated surface velocities ranging from about 0.1 - 0.2 m/s for a similar system considered here.(16)

An important point to be made about the temperature field is that the average temperature of 1650°C agrees well with the measurements.

The examination of the temperature field is instructive, because it shows that a temperature difference of about 10°C may exist even in this relatively small scale system, in spite of regions having quite high linear velocities. This is a significant finding which deserves further comment.

The apparently quite rapid circulation rates that were predicted do not guarantee that the system is well mixed, provided the time scale for convection is much smaller than the diffusive time scale.

For the present case, t_c, the convective time scale is given as:

$$t_c \approx \frac{d}{U} \approx 0.02 \text{ s} \qquad (38)$$

while the diffusive time scale (for turbulent flow) is given as:

$$t_{d,H} = \frac{d^2}{\alpha_{eff}} \approx 1 \text{ s} \qquad (39)$$

This can explain the existence of the slight temperature gradients within the system. The question of mixing is of greater importance in diffusion problems (since the molecular diffusivity for molten metals is much smaller than the thermal diffusivity, even when both are effectively enhanced by turbulence) and this question will be discussed subsequently.

Fig. 9 shows a computed plot of both the turbulent kinetic energy and of the ratio: effective viscosity/molecular viscosity for the system. The important point to note here is that k is sharply reduced and that the ratio μ/μ_{eff} tends to a value of 2 on approaching the free surface. It has to be stressed that this behavior has not been externally imposed on the system, but rather is a direct consequence of the curvi-linear geometry employed here. More specifically the rate of energy transfer from the center toward the outside is being diminished by the generation of angular momentum. Another important factor, which contributes to the laminarization of the flow field close to the free surface, is the energy consummed in the acceleration of the fluid in this region. [17]

It should be noted, that yet another factor, which may contribute to the laminarization of the flow field in the vicinity of the free surface, is the role played by surface tension forces. This effect has not been considered explicitly in this formulation, but will be commented upon in the subsequent section of this paper.

4.4 Reaction Kinetics in a Levitated Droplet

The previously given computed results were found to be in good quantitative or at least semi-qualitative agreement with measurements, regarding the lift force, the surface velocities and the mean temperature. Examination of the computed temperature field has indicated that the system was not very well mixed, in spite of the quite rapid circulation rates, but no direct experimental evidence was available to support these predictions.

Much better insight regarding the extent of mixing in the system may be obtained by the re-examination of some kinetic measurements reported by El-Kaddah and Robertson.[15]

In this work the rate of carburization of iron droplets was studied with a CO_2/CO mixture, for experimental conditions which have been given previously.

The carburization reaction involved the following reaction scheme.

$$2CO \rightleftharpoons CO_2 + (C)_{Fe} \qquad (40)$$

Previous studies have shown that the chemical reaction rate was very fast under the experimental conditions employed, furthermore, the calculated gas phase mass transfer rate was found to be faster than the experimentally observed rates. It follows that the rate limiting step had to be liquid phase diffusion or a mixed control involving both the gaseous and the motion phases.

On postulating mixed control the governing equations take the following form:

conservation of the transferred species:

$$\frac{\partial C}{\partial t} + \frac{1}{r^2}\left(\frac{\partial}{\partial r}\rho U_r^2 C\right) - r^2 \left(\frac{\mu}{Sc_\ell} + \frac{\mu_t}{Sc_t}\right)\frac{\partial C}{\partial r}\Big) + \frac{1}{r \sin\theta}$$

$$\frac{\partial}{\partial\theta}\left(\rho U_\theta \sin\theta\, C - \frac{\sin\theta}{r}\left(\frac{\mu}{Sc_\ell} + \frac{\mu_t}{Sc_t}\right)\frac{\partial C}{\partial\theta}\right) = 0 \qquad (41)$$

the boundary conditions are given as follows:

$$C = 0 \quad \text{at} \quad t = 0 \qquad (42)$$

specifying zero initial carbon content, and,

$$\left(\frac{\mu}{Sc_\ell} + \frac{\mu_t}{Sc_t}\right)\frac{\partial C}{\partial r}\Big|_{r=R} = k_g \left(X_{CO_2{}_s} - X_{CO_2{}_B}\right) \qquad (43)$$

specifying the continuity of the flux of carbon of the gas-melt interface where $X_{CO_2{}_s}$ is calculated from equilibrium considerations and may be expressed as

$$X_{CO_2} = 1 + \frac{K\ a_c}{2P} - \sqrt{\left(1 + \frac{K a_c}{2P}\right)^2 - 1} \qquad (44)$$

where the activity of carbon is given by [18]

$$a_c = \underline{C}\ 10^{\cdot 1\underline{C}} \qquad (45)$$

This system of equations is readily solved, utilizing the previously obtained values of the velocity field and of the turbulence parameters, needed to compute the values of the eddy diffusivity.

In view of the sharp changes in both the eddy diffusivity and in the volume of the grids in the vicinity of the free surface a somewhat finer grid structure was used in these calculations, employing 17x16 grids, with the extra points being located in the vicinity of the free surface.

Fig. 10 shows the experimental measurements with the full circles; the computed results, using turbulent flow considerations are given by the broken line, while the solid line shows the results of calculations, assuming laminar flow in the levitated sphere.

It is seen that the assumption of laminar flow gave excellent agreement between the measurements and the predictions. The calculated results based on turbulent flow appear to be quite close also, but this may be somewhat misleading, because the curve drawn with the broken line closely approaches the limit of gas phase mass transfer control.

These results clearly indicate substantial damping of the turbulence in the vicinity of the free surface, which appears to go well beyond the behavior that was attributable to the acceleration of the flow and the curvi-linear coordinate system that were discussed earlier.

Mechanisms that may be responsible for the damping of turbulence in the vicinity of the free surface may include the role played by surface tension forces, as discussed by Levich[19] and Davis[20]. However another important mechanism that may have to be considered is the damping of the turbulence by the electromagnetic field, which would be particularly important in damping the velocity components parallel to the free surface.[21]

In view of the quasi-laminar behavior postulated in the vicinity of the free surface it may be of interest to show one additional figure, depicting the computed velocity field and temperature field for laminar flow conditions. This is done in Fig. 11 where it is seen that the behavior is qualitatively similar

to that found for turbulent flow, except for the fact that the linear velocities are some 30-40% higher and the isotherms are consistent with a rather well defined laminar circulation pattern.

5. CONCLUDING REMARKS

A mathematical representation has been developed for the electromagnetic force field, the fluid flow field, temperature field and transport controlled kinetics in a levitated metal droplet.

The statement of the problem included the use of mutual inductances to calculate the current density distribution in the droplet resulting from a given coil currentand coil configuration. Knowledge of the current density distribution enabled the calculation of the lifting force, of the stirring force within the sphere and of the heat generation pattern.

The fluid flow field in the sphere was modelled by writing the turbulent Navier-Stokes equations in spherical coordinates, with symmetry about the angle 0. The effect of both buoyancy and electromagnetic forces was included in the formulation, thus the fluid flow equations were coupled with the differential thermal energy balance equation, which included convection, eddy conduction and heat generation. A differential component balance was also developed to represent the carburization of an iron sphere, due to the decompesition of CO at the metal surface. The governing equations were solved numerically, using the k-ε model for the turbulent viscosity and employing primitive variables.

Computed results were obtained for the lifting force, for the

heat generation pattern, the velocity and temperature fields and the rate of carburization. The theoretical predictions were compared with experimental measurements, reported previously.

In a macroscopic sense the theoretically predicted lifting force and mean bulk temperature of the levitated sphere were found to be in good agreement with the measurements.

It is thought, however that the detailed insight into the microscopic behavior of the system, provided by these calculations was perhaps of greater significance.

The calculations have shown that the electromagnetic force field in the molten metal sphere produced quite high melt velocities, of the order of 0.1 - 0.3 m/s; these values were in qualitative agreement with the estimates deduced from the visual observation of levitated specimens. While the fluid flow field was definitely turbulent in the central part of the sphere, notwithstanding the quite small linear scale of the system, laminarization had occurred to a considerable extent in the vicinity of the free surface.

In a mathematical sense this laminarization is attributable to the acceleration of the fluid in a curvi-linear system. In a physical sense laminarization near the free surface may also have been promoted by surface tension forces.

This laminarization of the flow field has important consequences regarding other transport phenomena. The calculated temperature fields within the sphere have shown that a certain non-uniformity of the temperatures may exist within the system (say temperature differences of up to 10°C in the particular case calculated)

notwithstanding the high linear fluid velocities and the relatively small physical size of the specimen (6mm diameter).

This laminarization has an even greater influence on transport controlled kinetics. In this regard the theoretical predictions for the rate of carburization were compared with experimental measurements. The theoretical predictions were based on the assumption that gas phase mass transfer and liquid phase convective (including turbulent) diffusion being the rate controlling factors. It was found that the use of a turbulent model would have over-predicted the carburization rates, while the postulate of laminar flow gave very good agreement between measurements and predictions. This latter finding clearly confirmed the important laminarizing effect of surface tension in the vicinity of the free surface, which in the present case corresponded to the major part of the physical domain.

At this stage it ought to be mentioned that two assumptions implicitly made in the formulation, namely spherical geometry and the absence of surface tension driven flows may be justified a posteriori by the reasonable agreement between the measurements and the predicted behavior. The close approximation to spherical geometry has been observed by many investigators, furthermore, the absence of significant temperature gradients on the surface should preclude significant surface tension driven flows, especially as the electromagnetic forces are at maximum at the free surface.

In conclusion it may be stated that a realistic mathematical representation has been developed for the electromagnetic force field

heat, mass and momentum transfer in levitated metal droplets and that the theoretical predictions appear to be in very good agreement with measurements.

It is suggested that these results may gain useful application in two distinct areas. One of these is the rational planning and interpretation of space processing experiments, which involve levitation melting. The other provides a potentially very useful tool for the interpretation of ground based levitation experiments, through the quantitative definition of the fluid flow field in these systems.

From the standpoint of basic fluid dynamics the laminarization of the flow field in the vicinity of the free surface is a very interesting finding, which will deserve further detailed study.

ACKNOWLEDGEMENTS

The authors wish to thank the National Aeronautics and Space Administration for support of this investigation through Grant-7645 given to the Materials Processing Center at MIT. Thanks are also due to Drs. C.W. Chang and T. Frost of the General Electric Co., Space Science Center, Valley Forge, PA for providing the program for calculating the electromagnetic force field.

LIST OF SYMBOLS

a_c activity of carbon

$\underset{\sim}{A}$ vector potential (Wb/m)

$\underset{\sim}{B}$ magnetic flux density (Wb/m^2)

B_a applied magnetic flux density (Wb/m^2)

$\underline{C}$ carbon concentration (Wt%)

C concentration diffusing species (kg/m^3)

C_p specific heat of levitated sphere (J/kg^oK)

C_1, C_2, C_μ constants of k-ε model (m)

$\underset{\sim}{E}$ electric field (v/m)

$\underset{\sim}{F}_\ell$ electromagnetic lifting force (N)

g gravitional acceleration (m/s^2)

$\underset{\sim}{F}_S$ electromagnetic stirring force (N/m^3)

h heat transfer coefficient $WW/m^{2o}K$)

I coil current (A)

Im imaginary value of

$\underset{\sim}{J}$ induced eddy current density (A/m^2)

$\tilde{k}$ turbulent kinetic energy (m^2s^2)

k_g mass transfer coefficient (m/s)

m mass of levitated drop (kg)

$M_{i,j}$ mutual inductance (H) levitated drop (W)

p power adsorbed by Eq. 22)

P pressure (N/m^2)

$\bar{P}$ modified pressure

r radial coordinate (m)

Re real value of

S cross sectional area of elementary circuit (m^2)

T temperature (^oK)

T_g ambiant gas temperature (^oK)

t time (s)

U velocity (m/s)

x	mole fraction of reactive gases
μ_o	magnetic permeability (H/m)
μ_t	turbulent viscosity (kg/m.s)
ρ	density of levitated sphere (kg/m^3)
ε	turbulent kinetic energy ($m^2 s^3$)
ε	emissivity of levitated sphere
σ	electric conductivity of levitated droplet $(\Omega m)^{-1}$
σ	Stefan-Boltzman constant ($J/s.m^2\ {}^oK^4$)
$\sigma_k \sigma_\varepsilon$	constants in k-ε model
ν	kinematic viscosity (m^2/s)
ω	frequency
α_{eff}	effective thermal diffusivity
α	thermal expansion coefficient

Dimensionless group

Nu	Nussett number
Pr	Prandtl number
Re	Reynolds number
Re_T	turbulent Reynolds number
Sc	Schmidt number
Gr	Grashof number

Figure Captions

1. Sketch of the levitation coil used in this work.
2. Sketch of the electromagnetic field in levitated sphere.
3. Illustration of the elementary circuit used in numerical computation.
4. Computed lifting force and power adsorption for a molten iron droplet along the axis of the coil. Coil current 200 Amp.
5. Computed lifting force and power adsorption for a molten iron droplet along the axis of the coil. Coil current 250 Amp.
6. Computed lifting force and power adsorption for a molten iron droplet along the axis of the coil. Coil current 300 Amp.
7. Computed electromagnetic force field and computed Joule heating ($x10^6$ W/m^3) in a levitated molten iron droplet. Coil current 250 Amp.
8. Computed velocity field and temperature field in a levitated iron sphere.
9. Computed turbulent kinetic energy ($x10^4.m^2/s^2$) RHS and the ratio of μ_{eff}/μ_ℓ LHS.
10. Experimental carburization results (CO 2.15/CO_2 at 38.9 atm and 1650°C) (13,15) compared with the theoretical predictions for turbulent and laminar flow in the levitated drop.
11. Computed velocity field and temperature field in a levitated molten drop assuming laminar flow.

REFERENCES

1. A.E. Jenkins, B. Harris and L.A. Baker, Symposium on metallurgy at high pressures and high temperatures, Met. Soc. AIME Conf. (1963), 22, p 23.
2. E.C. Okress, D.M. Wroughton, G. Comenetz, P.H. Brace and J.C.R. Kelly, J. Appl. Phy. (1952), 23, 545.
3. J. Szekely and C.W. Chang, Ironmaking ans Steelmaking, (1977), 4, 190.
4. J. Szekely and C.W. Chang, Ironmaking and Steelmaking, (1977) 4, 196.
5. E. Tarapore and J. Evans, Met. Trans. B, (1976), 7B, 343.
6. P. Cremer, Dr. Ing. Thesis, Universite de Grenoble, France, (1979).
7. M. Choudhary and J. Szekely, Met. Trans. B, (1980), 11B, 439.
8. W.K.H. Panofsky and M. Phillips, Classical Electricity and Magnetism, 2nd edition, (1962), Addison-Wesley.
9. B.E. Launder and D.B. Spalding, Math. Models of Turbulence, Academic Press (1972).
10. B.E. Launder and D.B. Spalding, Computer Meth. Appl. Mech. Engr. (1974), 3, 269.
11. M. Choudhary, J. Szekely, B.I. Medovar, Y.G. Emelyanenko, Met. Trans. B. (1982), 13B, 35.
12. N. E.-Kaddah and J. Szekely, J. Fluid Mech. in press.
13. N.H. El-Kaddah, Ph.D. Thesis, Imperial College, London, (1976).

14. D.B. Spalding, Basic Equations of Fluid Mechanics, and Heat and Mass Transfer, and Procedures for their Solution, Report HTS 17616, Imperial College, London, (1976).

15. N.M. El-Kaddah and D.G.C. Robertson, Met. Trans. B, (1978), 9B, 191.

16. D.G.C. Roberson and A.E. Jenkins, Heterogeneous Kinetics at Elevated Temperature, ed. Plenum Press, (1970), p 393

17. P. Bradshaw, Effects of Steamline Curvature on Turbulent Flow, (1973), AGAR Dograph 169.

18. N.H.El-Kaddah and D.G.C. Robertson, Met. Trans. B, (1977), 8B, 569.

19. V. G. Levich, Physicochemical Hydro-dynamics, Prentice-Hall Inc. (1962).

20. J.T. Davies, Turbulence Phenomena, Academic Press. (1972).

21. H. Branover and P. Gershon, Symp. on Turbulent Shear Flows, (1977), Univ. Park Pennsylvania.

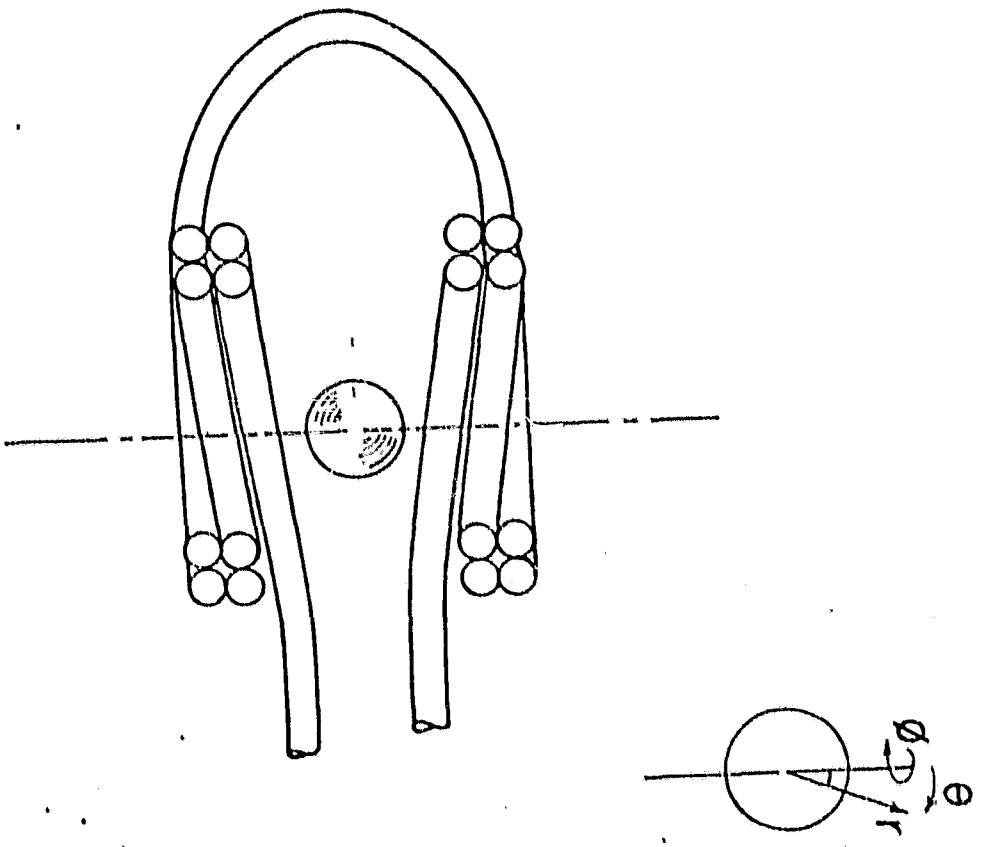

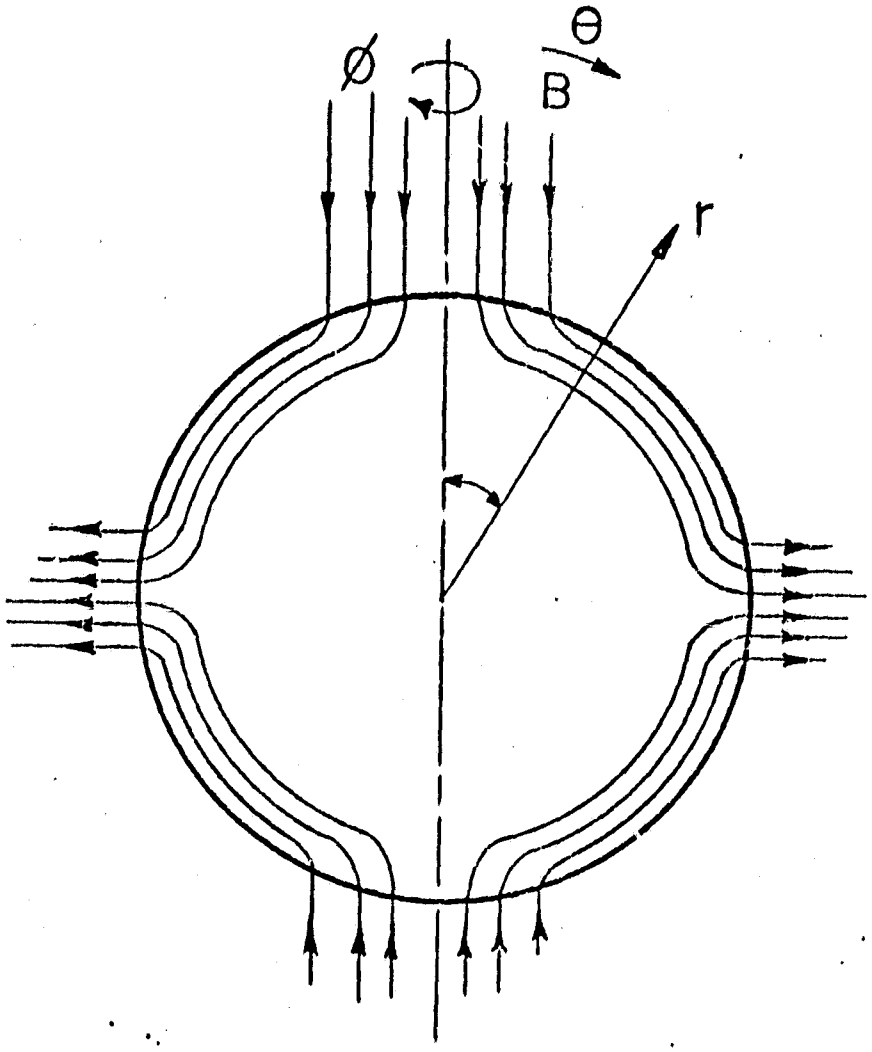

Fig (4)

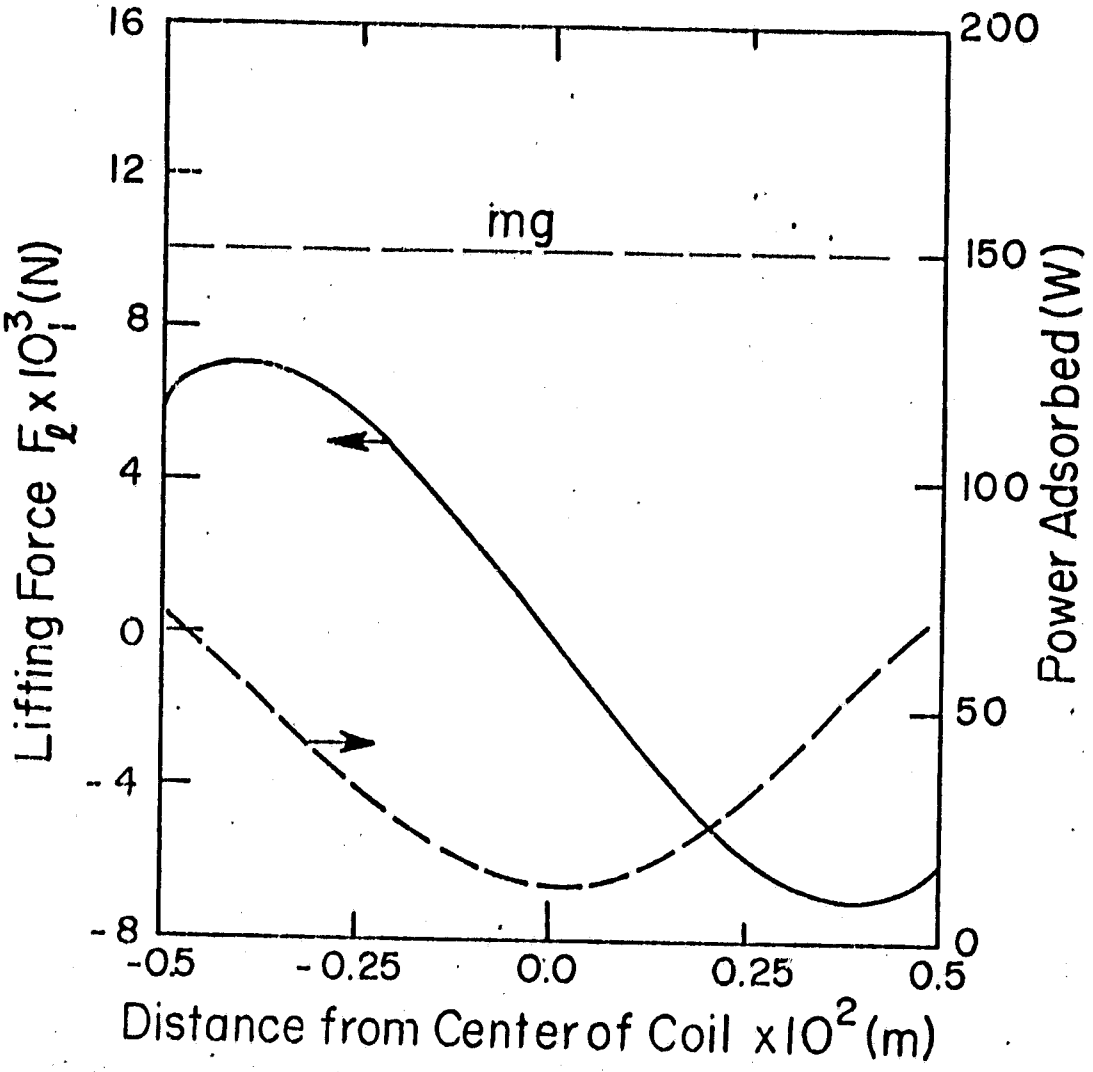

ORIGINAL PAGE IS
OF POOR QUALITY

Fig (5.1)

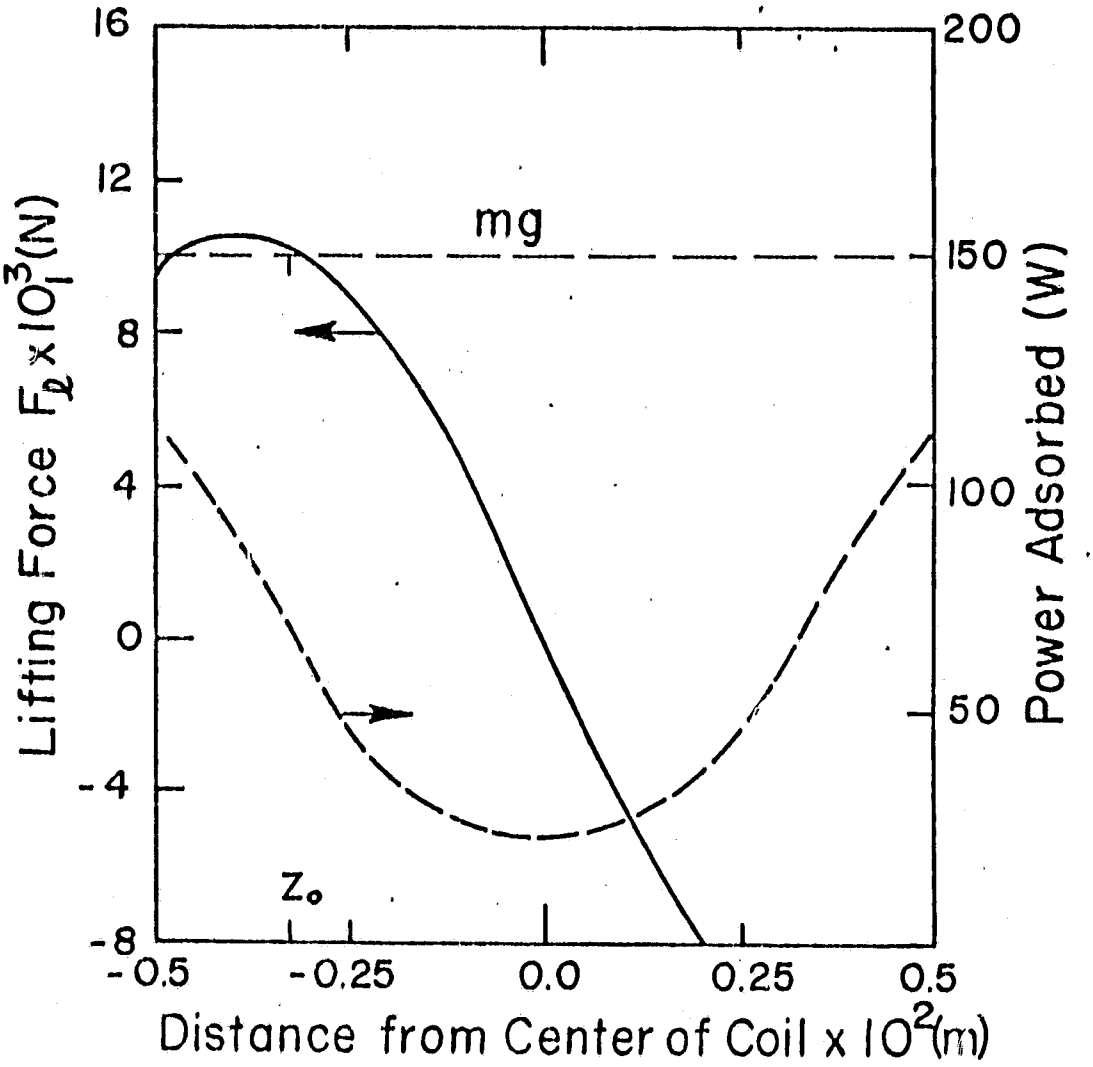

Fig(6)

ORIGINAL PAGE IS
OF POOR QUALITY

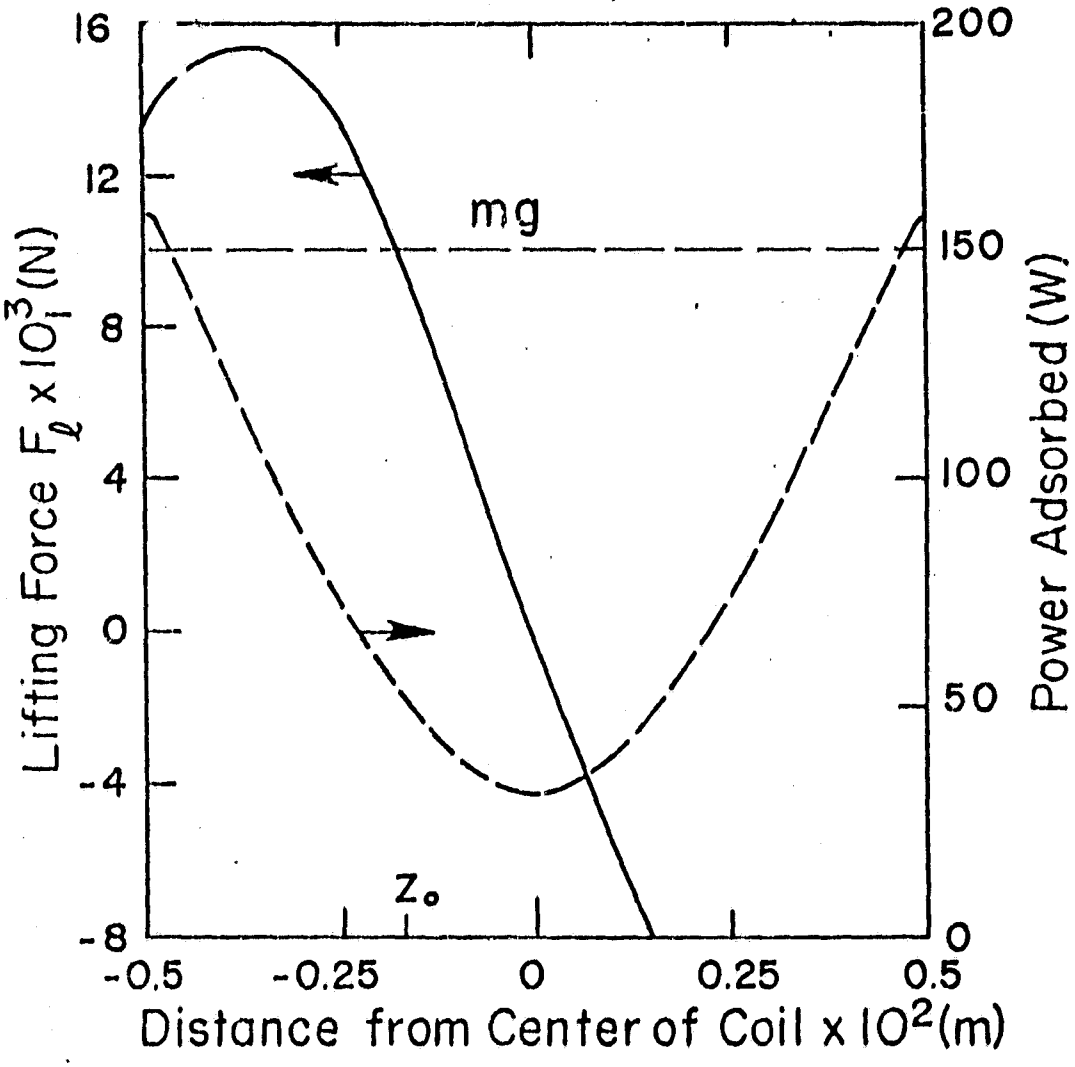

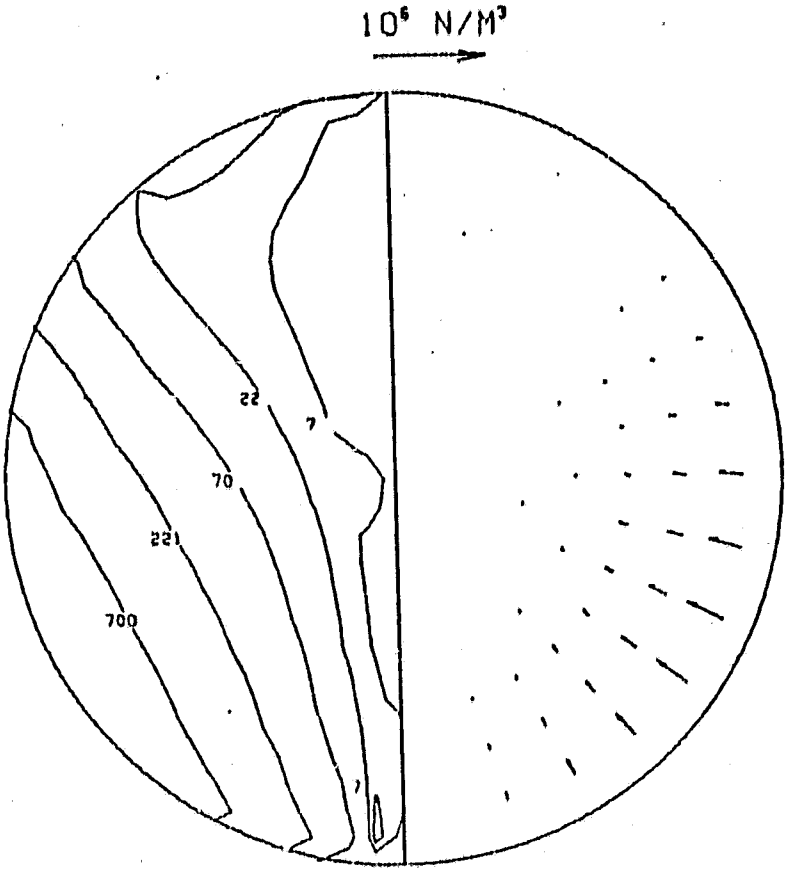

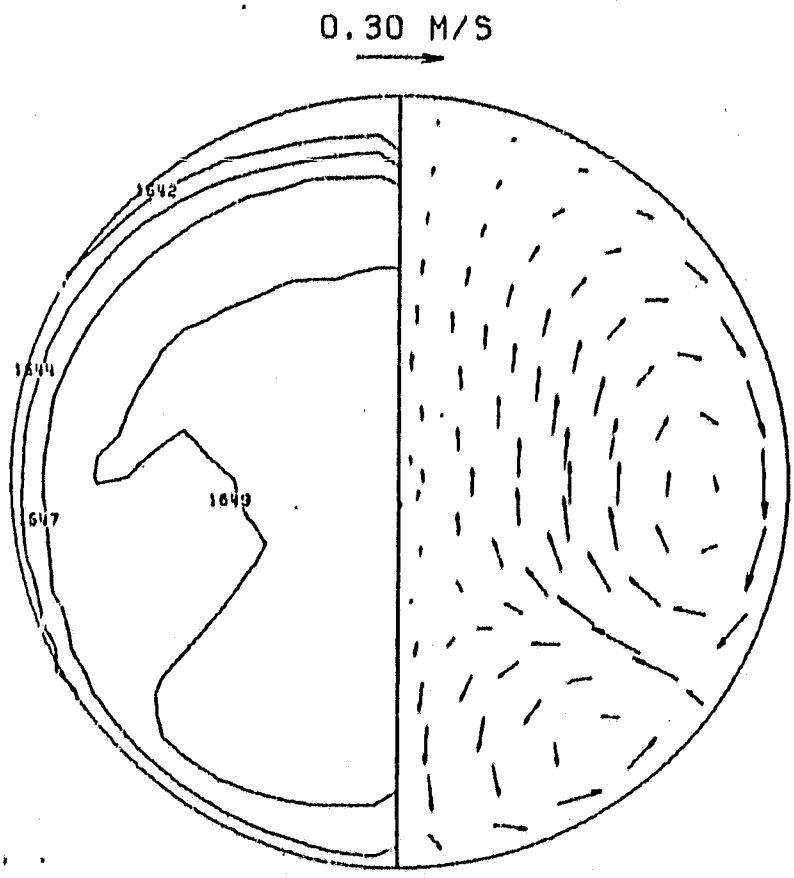

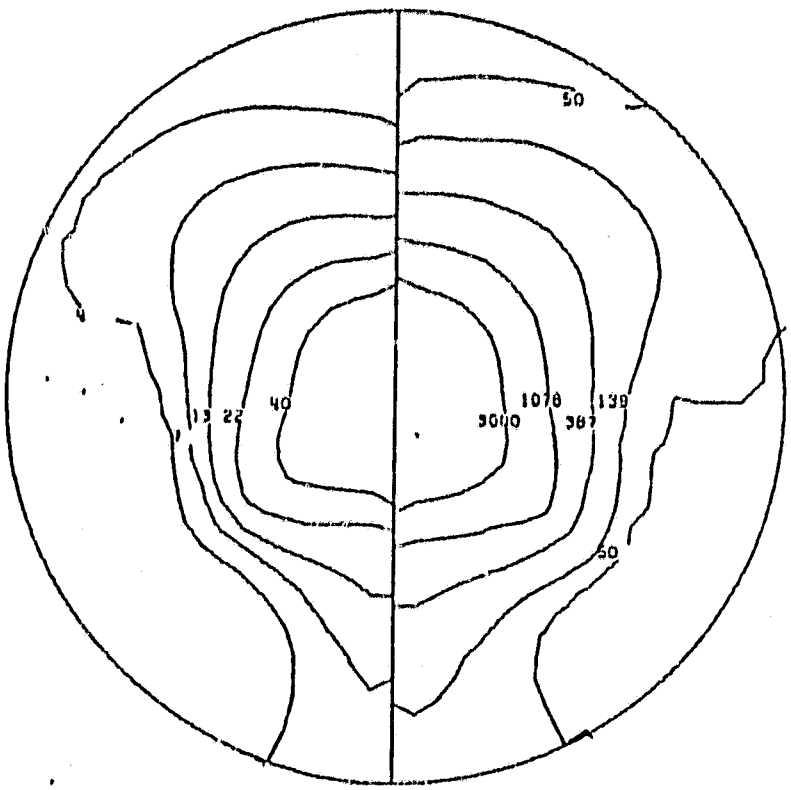

Fig (10)

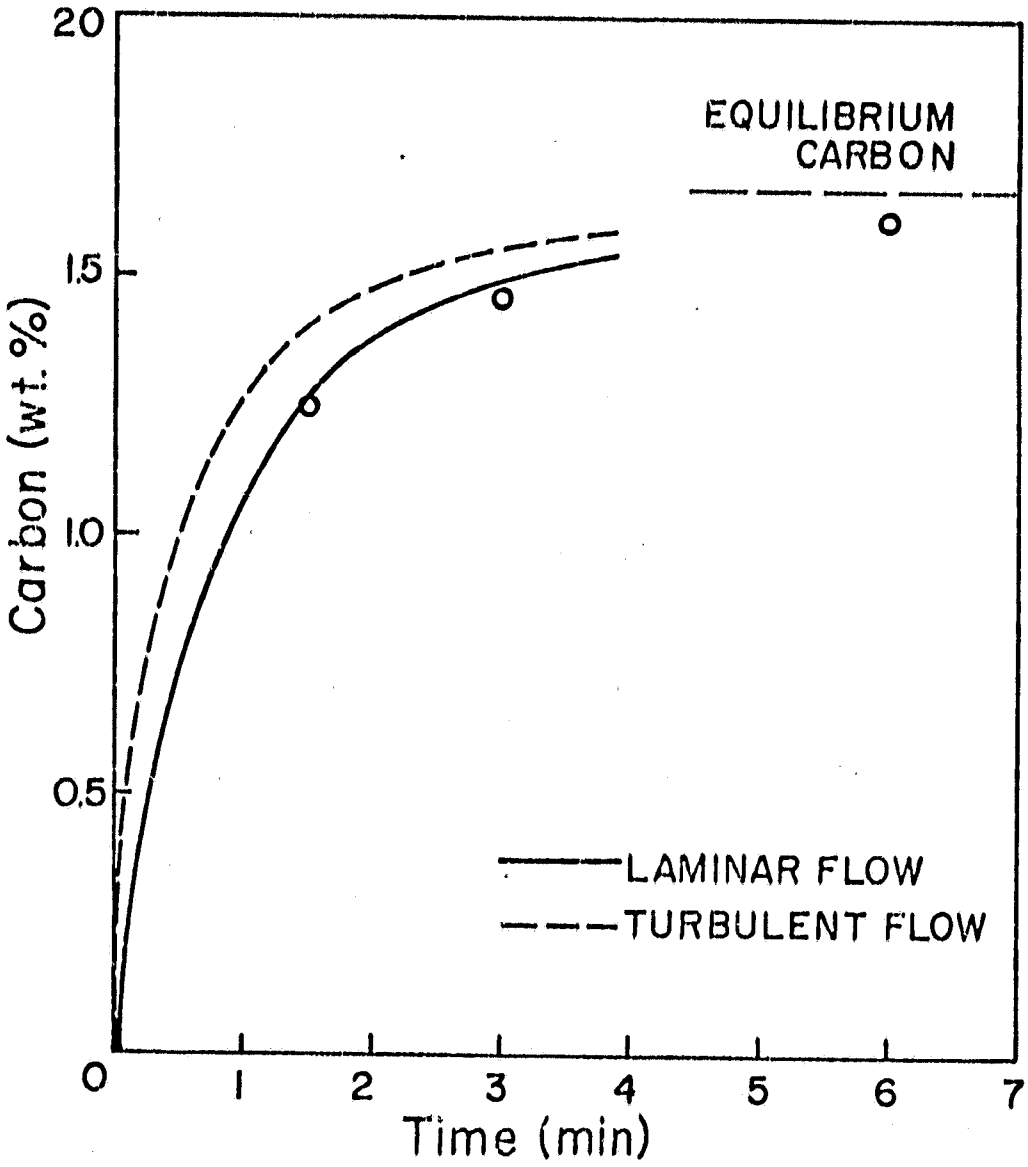

(11)

ORIGINAL PAGE IS
OF POOR QUALITY